Journal of Magnetism and Magnetic Materials 324 (2012) 2706–2710

Contents lists available at SciVerse ScienceDirect

Journal of Magnetism and Magnetic Materials

journal homepage: www.elsevier.com/locate/jmmm

Green's function study of a mixed spin-1 and spin-3/2 Heisenberg ferrimagnetic system

Gülistan Mert *

Department of Physics, Selçuk University, 42075 Kampüs Konya, Turkey

ARTICLE INFO

Article history:
Received 11 September 2011
Received in revised form
4 February 2012
Available online 27 March 2012

Keywords:
Heisenberg ferrimagnetic system
Green's function
Critical temperature
Compensation temperature
Single-ion anisotropy

ABSTRACT

The magnetic properties of a mixed spin-1 and spin-3/2 Heisenberg ferrimagnetic system on a square lattice are investigated by using the double-time temperature-dependent Green's function technique. In order to decouple the higher order Green's functions, Anderson and Callen's decoupling and random phase approximations have been used. The nearest- and next-nearest-neighbor interactions and the single-ion anisotropies are considered and their effects on compensation and critical temperature are studied.

1. Introduction

The ferromagnetic materials are mainly characterized by their compensation temperature, at which the total magnetization vanishes while sub-lattice magnetizations do not. These properties of ferromagnetic materials are extremely important in theoretical applications mainly in magnetic recordings. The models may assist in an understanding of features of same two- and three- dimensional bimetallic molecular ferrimagnets [1].

In the last years, theoretical studies of the two sub-lattices mixed spin systems have increased. Many theoretical models have been used with different techniques. Especially, Nakamura and Tucker have used the Monte Carlo technique for studying a mixed spin-1 and spin-3/2 Ising ferromagnet [2]. Tucker has used the cluster variational theory for a mixed spin-1 and spin-3/2 Blume—Capel Ising ferromagnet [3]. O. F. Abubrig et al. have used the mean field approach for a mixed spin Ising system with different anisotropies [4]. Jiang et al. have studied the tricritical behavior and magnetic properties for a mixed Ising system with crystal field using an effective field theory which they have developed [5]. Albayrak has studied mixed spin-1 and spin-3/2 Ising ferromagnet on a Bethe lattice by using the exact recursion technique [6].

In this work, we have studied two sub-lattices ferrimagnetic Heisenberg system with spin-1 and spin-3/2 on a square lattice by using the double-time temperature-dependent Green's function technique, which is quite similar to that of J. Li et al. [7]. The outline of this paper is as follows. In Section 2, we give the model and fundamental equations. In Section 3, results and discussions are given. We illustrate the effects of the next-nearest-neighbor interactions and the single-ion anisotropies on compensation and critical temperature. Section 4 contains conclusions.

2. Model and Green's function formalism

Our main purpose is the evaluation of the averaged sub-lattice magnetizations m_A and m_B of sub-lattices A and B, respectively, defined as

$$m_A = \langle S_A^z \rangle, m_B = \langle S_B^z \rangle \tag{1}$$

The averages of square of the magnetizations are called the quadrupolar moments:

$$Q_A = \langle (S_A^z)^2 \rangle, Q_B = \langle (S_B^z)^2 \rangle \tag{2}$$

Let us consider the mixed spin-1 and spin-3/2 Heisenberg ferrimagnetic model on a square lattice divided into two equivalent sub-lattices A and B. Both sub-lattices are also square lattices. The distance between the nearest A and B atoms is taken as a. We assume the Hamiltonian as follows:

$$H = -\sum_{<\mathrm{nn}>} J_{ij} S_i S_j - \sum_{<\mathrm{nnn}>} J_{\mathrm{ii}'} S_i S_{i\not\in} - \sum_{<\mathrm{nnn}>} J_{\mathrm{jj}\not\in} S_j S_{j\not\in} - D_{\mathrm{A}} \sum_i (S_i^z)^2 - D_{\mathrm{B}} \sum_j (S_j^z)^2 \tag{3}$$

* Fax: + 90 332 2376195.
E-mail address: gmert@selcuk.edu.tr

0304-8853/$ - see front matter © 2012 Elsevier B.V. All rights reserved.
http://dx.doi.org/10.1016/j.jmmm.2012.03.033

where $\langle$ nn $\rangle$ and $\langle$ nnn $\rangle$ denote the nearest- and next-nearest-neighbors interactions, respectively. i belongs to sub-lattice A (spin-1), j belongs to sub-lattice B (spin-3/2). $J_{ij}=J$ (<0) is the antiferromagnetic exchange interaction between the nearest-neighbor spins $\boldsymbol{S}_i$ and$\boldsymbol{S}_j$, $J_{ii\acute{e}}=J_1$ (>0) is the ferromagnetic exchange interaction between the next nearest-neighbor spins $\boldsymbol{S}_i$ and $\boldsymbol{S}_{i\acute{e}}$ and $J_{jj\acute{e}}=J_2$ (>0) is the next ferromagnetic exchange interaction between the next nearest-neighbor spins $\boldsymbol{S}_j$ and $\boldsymbol{S}_{j\acute{e}}$. D_A is the anisotropy parameter of the sub-lattice A and D_B is that of the sub-lattice B.

We introduce the Green's functions $\langle\langle S_i^+;B_l\rangle\rangle_\omega$ and$\left\langle\left\langle S_j^+;B_l\right\rangle\right\rangle_\omega$, where $B_l=e^{\eta S_i^z}S_i^-$ and η is a parameter [8].

We have the following equations of motion for the Green's functions:

$$\omega\langle\langle S_i^+;B_l\rangle\rangle=\delta_{il}\langle[S_i^+,B_l]\rangle-J\sum_{<\mathrm{nn}>}\langle\langle(S_i^zS_j^+-S_i^+S_j^z);B_l\rangle\rangle -J_1\sum_{<\mathrm{nnn}>}\langle\langle(S_i^zS_{i\acute{e}}^+-S_i^+S_{i\acute{e}}^z);B_l\rangle\rangle+D_A\langle\langle(S_i^+S_i^z+S_i^zS_i^+);B_l\rangle\rangle \tag{4}$$

$$\omega\langle\langle S_j^+;B_l\rangle\rangle=\delta_{jl}\langle[S_j^+,B_l]\rangle-J\sum_{<\mathrm{nn}>}\langle\langle(S_j^zS_i^+-S_j^+S_i^z);B_l\rangle\rangle -J_2\sum_{<\mathrm{nnn}>}\langle\langle(S_j^zS_j^+-S_j^+S_j^z);B_l\rangle\rangle+D_B\langle\langle(S_j^+S_j^z+S_j^zS_j^+);B_l\rangle\rangle \tag{5}$$

where δ is the Dirac function and $\langle\ldots\rangle$ is the thermal average. We have taken the value of $\hbar$ as 1.

The higher order Green's functions can be decoupled as follows. The Green's functions coming from the exchange terms like $\langle\langle(S_i^zS_j^+-S_i^+S_j^z);B_l\rangle\rangle$ can be decoupled by using the random phase approximation (RPA) [9], that is

$$\langle\langle S_i^zS_j^+;B_l\rangle\rangle\cong\langle S_i^z\rangle\langle\langle S_j^+;B_l\rangle\rangle \tag{6}$$

The Green's functions coming from the single-ion anisotropy, like $\langle\langle(S_i^zS_j^+-S_i^+S_j^z);B_l\rangle\rangle$, cannot be decoupled by means of RPA, since the vertical and horizontal components of the spin operation on the same site are not independent any longer. These kinds of decoupling can be done by using Anderson and Callen's decoupling schema [10], that is

$$\langle\langle(S_i^+S_i^z+S_i^zS_i^+);B_l\rangle\rangle\cong\tau_A\langle\langle S_i^+;B_l\rangle\rangle \text{ and } \langle\langle(S_j^+S_j^z+S_j^zS_j^+);B_l\rangle\rangle\cong\tau_B\langle\langle S_j^+;B_l\rangle\rangle \tag{7}$$

where

$$\tau_A=\left\{2-\frac{1}{S_A^2}[S_A(S_A+1)-Q_A]\right\}m_A \text{ and } \tau_B=\left\{2-\frac{1}{S_B^2}[S_B(S_B+1)-Q_B]\right\}m_B \tag{8}$$

This decoupling schema is very satisfactory [11].

Then we obtain the following Green's function:

$$G_A(\omega,K)=\frac{\Theta_A(\eta)}{E^+-E^-}\left[\frac{\omega-C}{\omega-E^+}-\frac{\omega-C}{\omega-E^-}\right] \tag{9}$$

$$G_B(\omega,K)=\frac{\Theta_B(\eta)}{E^+-E^-}\left[\frac{\omega-A}{\omega-E^+}-\frac{\omega-A}{\omega-E^-}\right] \tag{10}$$

where

$$\Theta_A(\eta)=\langle[S_i^+,e^{\eta S_i^z}S_i^-]\rangle,\quad \Theta_B(\eta)=\langle[S_j^+,e^{\eta S_j^z}S_j^-]\rangle \tag{11}$$

$$E^\pm=\frac{1}{2}\left\{(A+C)\pm[(A-C)^2+4BD]^{1/2}\right\} \tag{12}$$

$$A=D_A\tau_A+4Jm_B-4J_1m_B(\gamma_2-1) \tag{13}$$

$$B=-4Jm_A\gamma_1 \tag{14}$$

$$C=D_B\tau_B+4Jm_A-4J_2m_B(\gamma_2-1) \tag{15}$$

$$D=-4Jm_B\gamma_1 \tag{16}$$

$$\gamma_1=\cos\left(\frac{\sqrt{2}}{2}k_xa\right)\cos\left(\frac{\sqrt{2}}{2}k_xa\right) \tag{17}$$

$$\gamma_2=\frac{1}{2}\left[\cos(\sqrt{2}k_xa)+\cos(\sqrt{2}k_xa)\right] \tag{18}$$

Using the spectral theorem and Callen's technique [8], we obtain sub-lattice magnetizations as

$$m_A=\frac{(S_A-\Phi_A)(1+\Phi_A)^{2S_A+1}+(S_A+1+\Phi_A)\Phi_A{}^{2S_A+1}}{(1+\Phi_A)^{2S_A+1}-\Phi_A{}^{2S_A+1}} \tag{19}$$

$$m_B=\frac{(S_B-\Phi_B)(1+\Phi_B)^{2S_B+1}+(S_B+1+\Phi_B)\Phi_B{}^{2S_B+1}}{(1+\Phi_B)^{2S_B+1}-\Phi_B{}^{2S_B+1}} \tag{20}$$

and quadrupolar moments for sub-lattices A and B as

$$Q_A=(2\Phi_A+1)(1+\Phi_A)-\frac{S_A{}^2\Phi_A{}^{2S_A+1}-(1+S_A)^2(1+\Phi_A)^{2S_A+1}+2[S_A\Phi_A{}^{2S_A+1}+(1+\Phi_A)^{2S_A+1}(1+S_A)](1+\Phi_A)}{(1+\Phi_A)^{2S_A+1}-\Phi_A{}^{2S_A+1}} \tag{21}$$

$$Q_B=(2\Phi_B+1)(1+\Phi_B)-\frac{S_B{}^2\Phi_B{}^{2S_B+1}-(1+S_B)^2(1+\Phi_B)^{2S_B+1}+2[S_B\Phi_B{}^{2S_B+1}+(1+\Phi_B)^{2S_B+1}(1+S_B)](1+\Phi_B)}{(1+\Phi_B)^{2S_B+1}-\Phi_B{}^{2S_B+1}} \tag{22}$$

where

$$\Phi_A=\frac{2}{N}\sum_K\frac{1}{E^+-E^-}\left[\frac{E^+-C}{e^{\beta E^+}-1}-\frac{E^--C}{e^{\beta E^-}-1}\right] \tag{23}$$

$$\Phi_B=\frac{2}{N}\sum_K\frac{1}{E^+-E^-}\left[\frac{E^+-A}{e^{\beta E^+}-1}-\frac{E^--A}{e^{\beta E^-}-1}\right] \tag{24}$$

Total magnetization of the system is defined by

$$M=m_A+m_B \tag{25}$$

Eqs. (19)–(24) can be solved numerically.

3. Results and discussions

We have studied the effects of the nearest and next-nearest-neighbor interactions and the single-ion anisotropies on compensation and critical temperature. Critical temperature is defined as the temperature where total magnetization and all sub-lattice magnetizations all vanish. Compensation temperature is defined as the temperature where total magnetization vanishes but sub-lattice magnetizations have equal and opposite non-zero values. Compensation and critical temperature are determined from fundamental equations.

Firstly, let us study the behavior of magnetization curves in the ground state. At $T=0$ K, the factor $(e^{\beta E^+}-1)^{-1}$ is zero for $E>0$ and is -1 for $E<0$. In this case Eqs. (23) and (24) are written as follows:

$$\Phi_{A0}=\frac{2}{N}\sum_K\frac{E^--C}{E^+-E^-} \tag{26}$$

$$\Phi_{B0}=\frac{2}{N}\sum_K\frac{E^--A}{E^+-E^-} \tag{27}$$

We obtain the behavior of the magnetization curves at zero temperature by substituting Eqs. (26) and (27) in Eqs. (23) and (24). Fig. 1 shows the behavior of sub-lattice magnetization curves in the ground state. From Fig. 1, we see that sub-lattice magnetization is not saturated at absolute temperature.

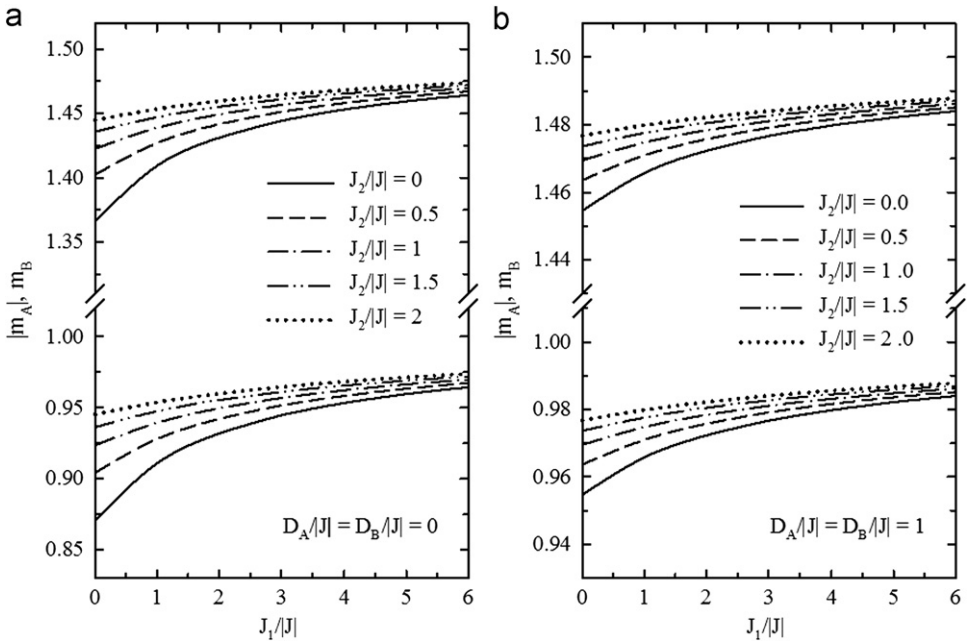

Fig. 1. Sub-lattice magnetizations versus $J_1/|J|$ of ground state for different values of $J_2/|J|$. (a) $D_A/|J|=D_B/|J|=0$ and (b) $D_A/|J|=D_B/|J|=1$.

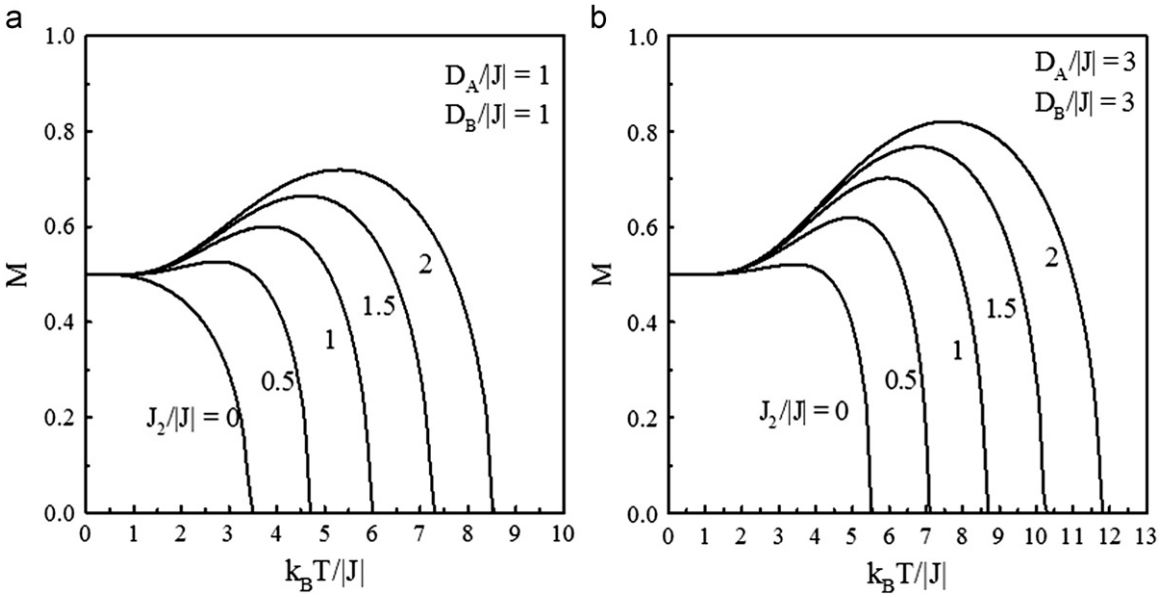

Fig. 2. Temperature dependence of total magnetization for different values of $J_2/|J|$ when $J_1/|J|=0$: (a) $D_A/|J|=D_B/|J|=1$ and (b) $D_A/|J|=D_B/|J|=3$.

It is a well-known fact that there exist zero point quantum fluctuations for spins at absolute zero. In addition, we see that as temperature decreases, zero-point fluctuation of spins decreases while the next-nearest-neighbor interactions and the single-ion anisotropies increase.

Fig. 2 shows the total magnetization curves for different values of $J_2/|J|$ at $J_1/|J|=0$ when $D_A/|J|$ and $D_B/|J|$ have constant values. As seen by these figures, there is no compensation point. In Fig. 2(a), we observe two types of magnetizations. In the absence of the next-nearest-neighbor interactions, the magnetization curve is of Q-type; when the next-nearest-neighbor interaction is taken into account the magnetization curves are of P-type according to Néel's classifications [12]. In Fig. 2(b), all of the magnetization curves are of P-type. Note that compensation temperature does not exist when the next-nearest-neighbor interactions are not included for $D_A/|J|=D_B/|J|=1$ and $D_A/|J|=D_B/|J|=3$. This result is different from that of the Ising system [13]. In the Ising system, when only nearest-neighbor interaction and the single-ion anisotropies are included, there is compensation temperature.

In Fig. 3, the total magnetizations are drawn. Fig. 3(a) shows the total magnetization curves when $J_1/|J|=3$, 4 and 5 for $J_2/|J|=0$, $D_A/|J|=1$ and $D_B/|J|=1$. When $J_1/|J|$ exceeds a certain minimum value ($J_{1\min}/|J|$), compensation points appear. The critical temperature increases with the increasing of $J_1/|J|$. Fig. 3(b) shows the total magnetization curves when $J_1/|J|=3$, 4 and 5 for $J_2/|J|=0$, $D_A/|J|=3$ and $D_B/|J|=3$. Similarly, compensation points appear when $J_1/|J|$ exceeds a certain minimum value ($J_{1\min}/|J|$). Critical temperature increases while compensation

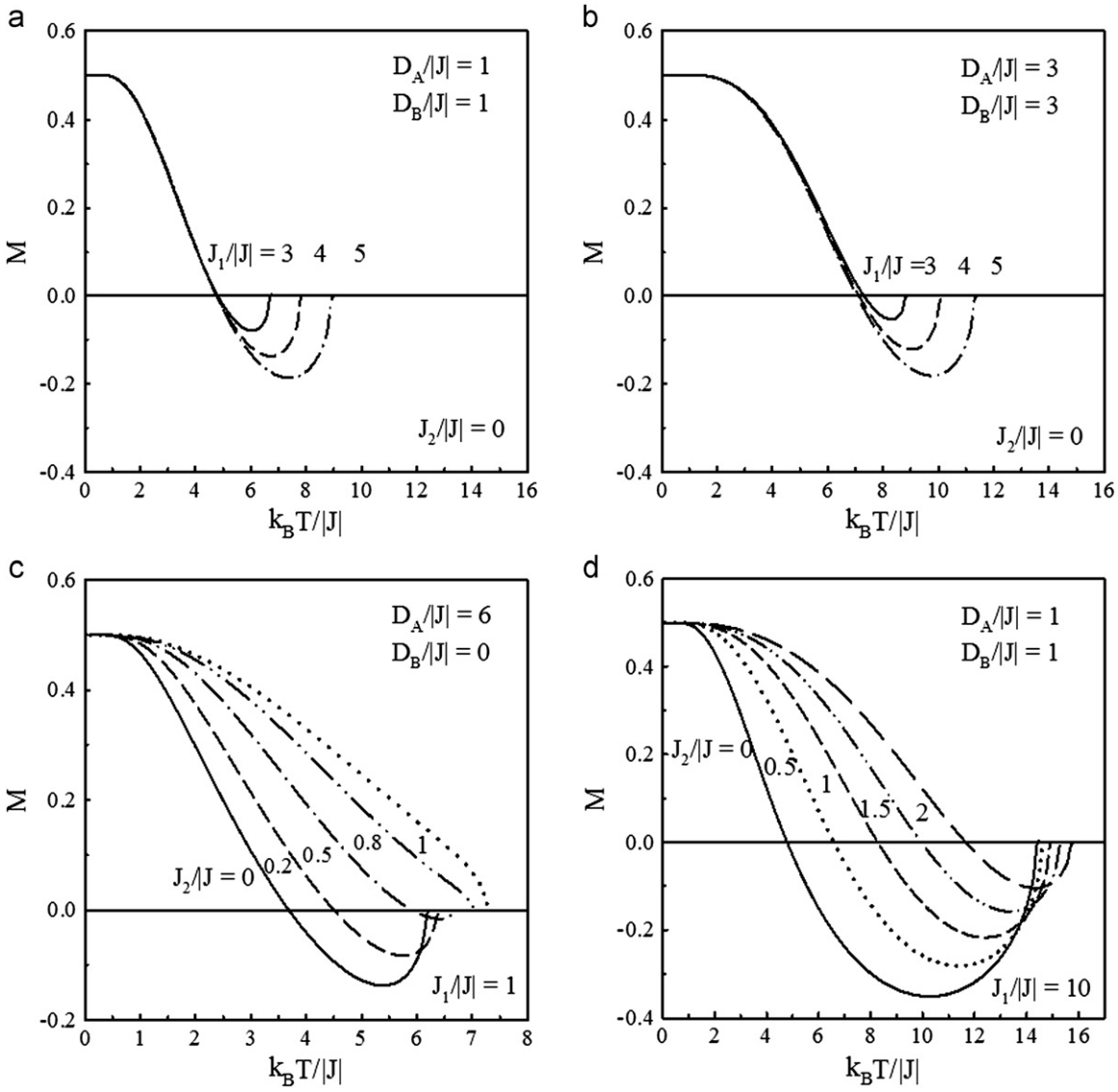

Fig. 3. Temperature dependence of total magnetization (a) for different values of $J_1/|J|$ when $J_2/|J|=0$, $D_A/|J|=1$ and $D_B/|J|=1$, (b) for different values of $J_1/|J|$ when $J_2/|J|=0$, $D_A/|J|=3$ and $D_B/|J|=3$, (c) for different values of $J_2/|J|$ when $J_1/|J|=1$, $D_A/|J|=6$ and $D_B/|J|=0$ and (d) for different values of $J_2/|J|$ when $J_1/|J|=10$, $D_A/|J|=1$ and $D_B/|J|=1$.

temperature decreases with increasing $J_1/|J|$. As shown in Fig. 3(a) and (b), both critical and compensation temperatures increase with increasing $D_A/|J|$ and $D_B/|J|$ values. The effects of the next-nearest-neighbor interaction $J_2/|J|$ on compensation and critical temperature are plotted in Fig. 3(c) and (d). From Fig. 3(c), it is clear that the compensation point appears for the values $J_2/|J|=0$, 0.2 and 0.5 while compensation temperature disappears for the values $J_2/|J|=0.8$ and 1. Fig. 3(d) shows the total magnetization curves when $J_2/|J|=0$, 0.5, 1, 1.5 and 2 for $J_1/|J|=10$, $D_A/|J|=1$ and $D_B/|J|=1$. It is evident that both compensation temperature and critical temperature increase with increasing $J_2/|J|$.

In Fig. 4, we have drawn the compensation and critical temperatures as a function of $J_1/|J|$ when $J_2/|J|=0$, 0.5 and 1 for constant values $D_A/|J|$ and $D_B/|J|$. Every critical temperature curve intersects with the corresponding compensation curve. For constant values $D_A/|J|$ and $D_B/|J|$, critical temperature increases with increasing $J_2/|J|$ and $J_1/|J|$ while compensation temperature increases with increasing $J_2/|J|$ and decreases with increasing $J_1/|J|$. Both critical and compensation temperatures increase with increasing $D_B/|J|$.

Compensation and critical temperatures as a function of $J_2/|J|$ for different values of $J_1/|J|$ at $D_A/|J|=6$ and $D_B/|J|=0$ are shown in Fig. 5. As $J_2/|J|$ increases, compensation temperature increases towards critical temperature at a maximum value of $J_2/|J|$ ($J_{2max}/|J|$), compensation and critical temperature become identical and compensation points disappear for $J_2/|J|$ greater than $J_{2max}/|J|$. Moreover, compensation points superpose at $J_2/|J|=0$. Critical temperature increases with increasing $J_1/|J|$ and $J_2/|J|$.

Compensation and critical temperatures as a function of $D_B/|J|$ for different values of $J_2/|J|$ at $D_A/|J|=1$ and $J_1/|J|=5$ are shown in Fig. 6. The situation in Fig. 6 is similar to that of Fig. 5, except that compensation points do not superpose in Fig. 6. Compensation and critical temperatures decrease with increasing $J_2/|J|$.

4. Conclusion

We have used the double-time temperature-dependent Green's function technique to study the mixed spin-1 and spin-3/2 Heisenberg ferrimagnetic model on a square lattice. We have studied

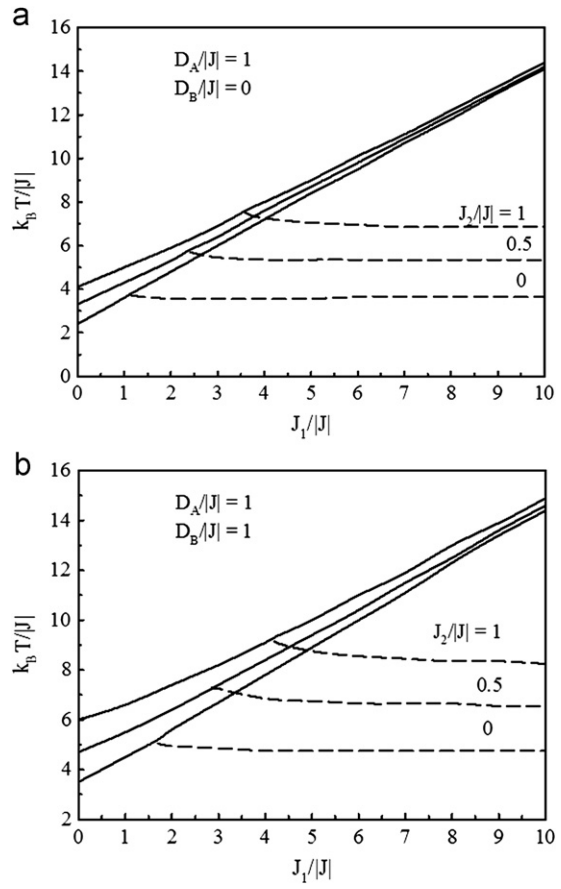

Fig. 4. Compensation and critical temperatures as a function of $J_1/|J|$ for different values of $J_2/|J|$ (a) at $D_A/|J|=1$ and $D_B/|J|=0$ and (b) at $D_A/|J|=1$ and $D_B/|J|=1$. The solid and dashed lines represent the critical and compensation temperatures, respectively.

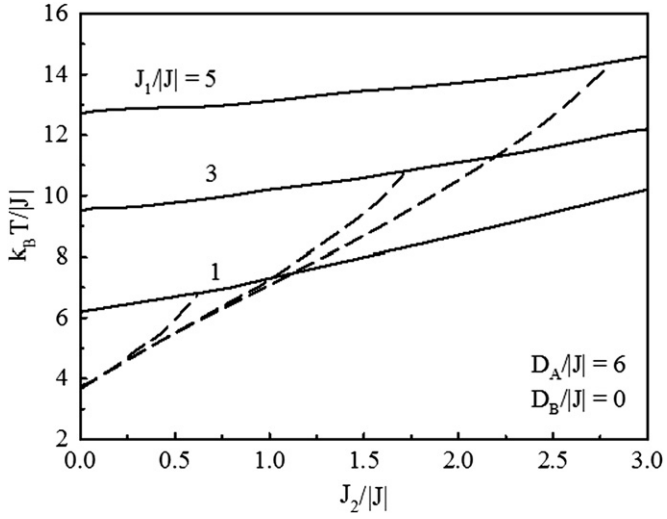

Fig. 5. Compensation and critical temperatures as a function of $J_2/|J|$ for different values of $J_1/|J|$ at $D_A/|J|=6$ and $D_B/|J|=0$. The solid and dashed lines represent the critical and compensation temperatures, respectively.

the effects of the nearest-and next-nearest-neighbor interactions and the single-ion anisotropies on the compensation and critical temperatures.

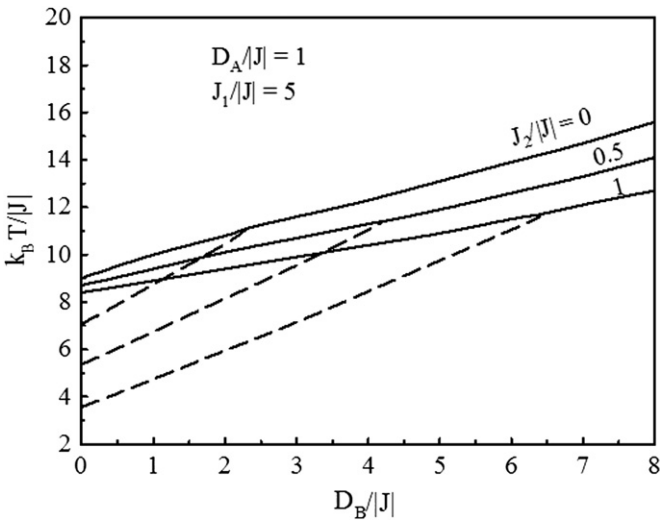

Fig. 6. Compensation and critical temperatures as a function of $D_B/|J|$ for different values of $J_2/|J|$ at $D_A/|J|=1$ and $J_1/|J|=5$. The solid and dashed lines represent the critical and compensation temperatures, respectively.

When only nearest-neighbor interaction and the single-ion anisotropies are included, there is no compensation point. In the absence of the next-nearest-neighbor interaction $J_1/|J|$, that is, when only $J_2/|J|$ is included, there is no compensation point. But when the next-nearest-neighbor interaction $J_2/|J|$ is not included, compensation point appears for $J_1/|J| \geq J_{1\min}/|J|$ values.

References

[1] A. Bobák, Physica A 258 (1998) 140.
[2] Y. Nakamura, J.W. Tucker, IEEE Transactions on Magnetics 38 (2002) 2406.
[3] J.W. Tucker, Journal of Magnetism and Magnetic Materials 237 (2001) 215.
[4] O.F. Abubrig, et al., Physica A 296 (2001) 437.
[5] Wei Jiang, Physical Review B 68 (2003) 134432.
[6] E. Albayrak, International Journal of Modern Physics B 17 (2003) 1087.
[7] J. Li, A. Du, G. Wei, Journal of Magnetism and Magnetic Materials 269 (2004) 410.
[8] H.B. Callen, Physical Review 130 (1963) 890.
[9] R.A. Tahir-Kheli, D. ter Haar, Physical Review 127 (1962) 88.
[10] F.B. Anderson, H.B. Callen, Physical Review 136 (1964) A1068.
[11] J.F. Devlin, Physical Review B 4 (1971) 136.
[12] L. Néel Ann., Physics Paris 3 (1948) 137.
[13] C. Ekiz, Journal of Magnetism and Magnetic Materials 307 (2006) 139.